GEOLOGICA CARPATHICA, FEBRUARY 2011, 62, 1, 43–53 doi: 10.2478/v10096-011-0004-0

Geomorphological, mineralogical, and geochemical evidence of Pleistocene weathering conditions in the southern Italian Apennines

PAOLA DI LEO[1], DARIO GIOIA[2], CLAUDIO MARTINO[2], ANNA PAPPALARDO[1] and MARCELLO SCHIATTARELLA[2]

[1]CNR — Istituto di Metodologie per l'Analisi Ambientale, Tito Scalo, 85050 Potenza, Italy; pdileo@imaa.cnr.it; apappalardo@imaa.cnr.it
[2]Dipartimento di Scienze Geologiche, Basilicata University, Campus Macchia Romana, 85100 Potenza, Italy; dario.gioia@unibas.it; claudio.martino@alice.it; marcello.schiattarella@unibas.it

(Manuscript received June 8, 2010; accepted in revised form December 20, 2010)

Abstract: Pleistocene weathering, uplift rates, and mass movements have been studied and correlated in a key-area of the Italian southern Apennines. The study area is the Melandro River valley, developed in a tectonically-controlled Quaternary intermontane basin of the axial zone of the chain. The goal of this paper is to assess ages and geomorphic features of two paleo-landslides and to relate them to values of uplift rates and the climate conditions in the axial zone of the chain during the Pleistocene. Uplift rates have been estimated using elevation and age of flat erosional land surfaces. In the southern area of the basin, the landscape features a wide paleo-landslide which can be ascribed to the upper part of the Lower Pleistocene on the basis of relationships with Quaternary deposits and land surfaces. Another paleo-landslide, in the northern sector of the basin, can be referred to the beginning of the Upper Pleistocene. The correlation between the ages of the two landslides and the temporal trend of the uplift rates allowed us to hypothesize that mass movements occurred in response to uplift peaks that destabilized slopes. Additionally, deciphering weathering conditions by means of the analysis of mineralogical and geochemical signals from landslide deposits and weathered horizons allowed assessment of changes in paleoclimate scenarios during the Pleistocene. The deep weathering was probably caused by the onset of warm-humid climate conditions, which may have acted as a further factor triggering landslide movements in an area already destabilized by the rapid uplift.

Key words: geomorphology, clay mineralogy, weathering indexes, Quaternary climate changes, Pleistocene landslides, southern Italy.

Introduction

Paleo-landslides in southern Italy have been largely studied from a geomorphological viewpoint, but their genetic relationships with tectonic activity, earthquakes, erosion base level modifications, climate changes, and weathering conditions are still debated. In particular, it seems hard to relate the development of huge ancient landslides to specific time intervals during the Quaternary in which one or more of the above mentioned mechanisms could have produced the necessary conditions for the activation of such significant phenomena. The targets of this study are: i) knowledge of the genetic links existing between ages, texture, weathered surfaces and geomorphic features of two Pleistocene large landslides located in an intermontane valley of southern Italy; ii) the correlation of these characteristics with the values of uplift rates from the study area and with the major episodes of climate change, as deduced from the global sea-level reconstruction. The comparison between these different data-sets is a useful tool for understanding the genetic mechanisms of landslides.

The investigated key-area is located in the Melandro River basin, a tectonic depression of the axial zone of the southern Apennines (Fig. 1). This chain constitutes a Neogene fold-and-thrust belt strongly uplifted and fragmented by neotectonics, and therefore characterized by many Quaternary longitudinal and transversal morphostructural depressions (Ortolani et al. 1992). Among them, the Melandro River basin is particularly suitable for the study of paleo-landslide generation by means of a geomorphological approach, because of the presence of both weathered erosional land surfaces and many morpho-structural markers which can be used for uplift rate estimates (Widdowson 1997). The interplay between climate and tectonics has long been considered a basic key for the interpretation of the landscape evolution at different scales (Bloom 1978; Ollier 1981; Bull 1991; Summerfield 2000; Burbank & Anderson 2001; Willett et al. 2006).

Geological and geomorphological features of the study area

The southern Apennines were strongly uplifted during the Quaternary, as shown by both Pleistocene displaced deposits and ancient base levels of erosion at high elevations above the present-day sea level (Schiattarella et al. 2003, 2006). The belt is in fact fragmented by Late Pliocene to Quaternary neotectonics (Schiattarella 1998), and therefore articulated by development of longitudinal and transversal tectonic depressions (Ortolani et al. 1992). The mountain belt tops are often charac-

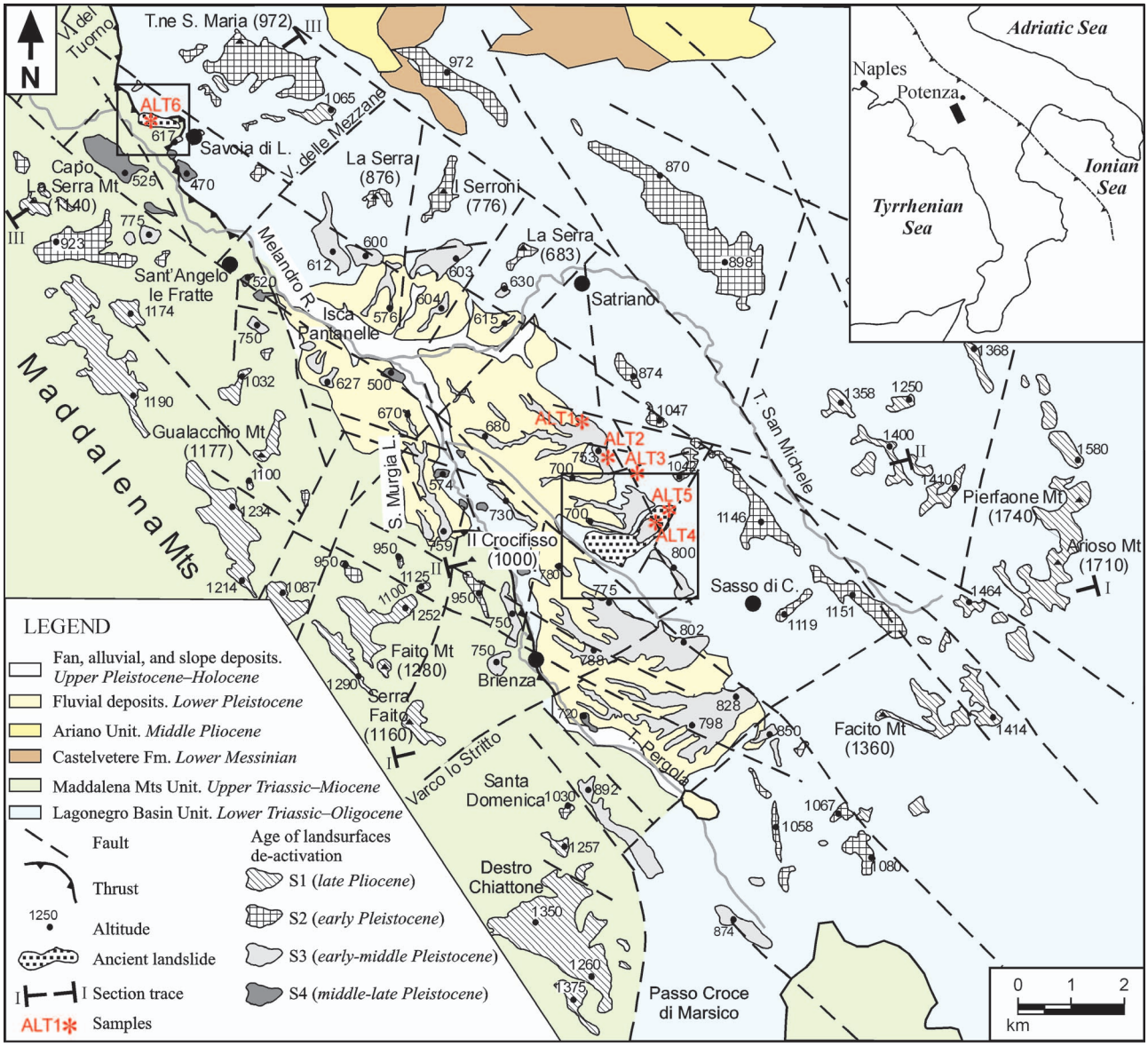

Fig. 1. Morphostructural map of the Melandro River basin (studied landslides in the frames).

terized by remnants of ancient erosional gently dipping or sub-horizontal land surfaces, hung with regard to the present-day base level of erosion due to Quaternary regional uplift and dismembered by multistage fault activity (Brancaccio et al. 1991; Amato & Cinque 1999; Schiattarella et al. 2003). Different Quaternary tectonic events have been recognized as responsible for the greatest part of the chain uplift. Several authors identified two main uplift stages in the Early Pleistocene, and another relevant event was marked by uplift that occurred in the Middle Pleistocene (D'Argenio et al. 1986; Brancaccio et al. 1991; Schiattarella et al. 2003). Finally, in the Late Pleistocene the chain was characterized by stability of the Tyrrhenian belt and uplift of the axial zone of the chain, the foredeep basin, and the foreland area (Westaway 1993; Bordoni & Valensise 1998; Schiattarella et al. 2003, 2006).

The Melandro River basin (Fig. 1) is a tectonic depression located in the "axial zone" of the chain (Ortolani et al. 1992). Two wide thrust sheets crop out in the area: the Maddalena Mts Unit and the Lagonegro units. The Maddalena Mts Unit is composed of Triassic to Eocene shallow-water carbonates locally covered by Upper Miocene siliciclastic sediments. It thrust up the Lagonegro units and forms the western flank of the basin, whereas the Lagonegro units, prevalently constituted by deep-sea successions, form the entire eastern side of the valley.

Alluvial deposits crop out in the axial zone of the Melandro River basin and have been attributed to the Early Pleistocene (Lippman Provansal 1987). Giano & Martino (2003) recognized three lithostratigraphic units separated by paleosols and erosional surfaces. Several generations of erosional surfaces have been identified on both sides of the valley (Fig. 1) and divided into four orders on the basis of geomorphological evidence (Schiattarella et al. 2003; Martino & Schiattarella 2006).

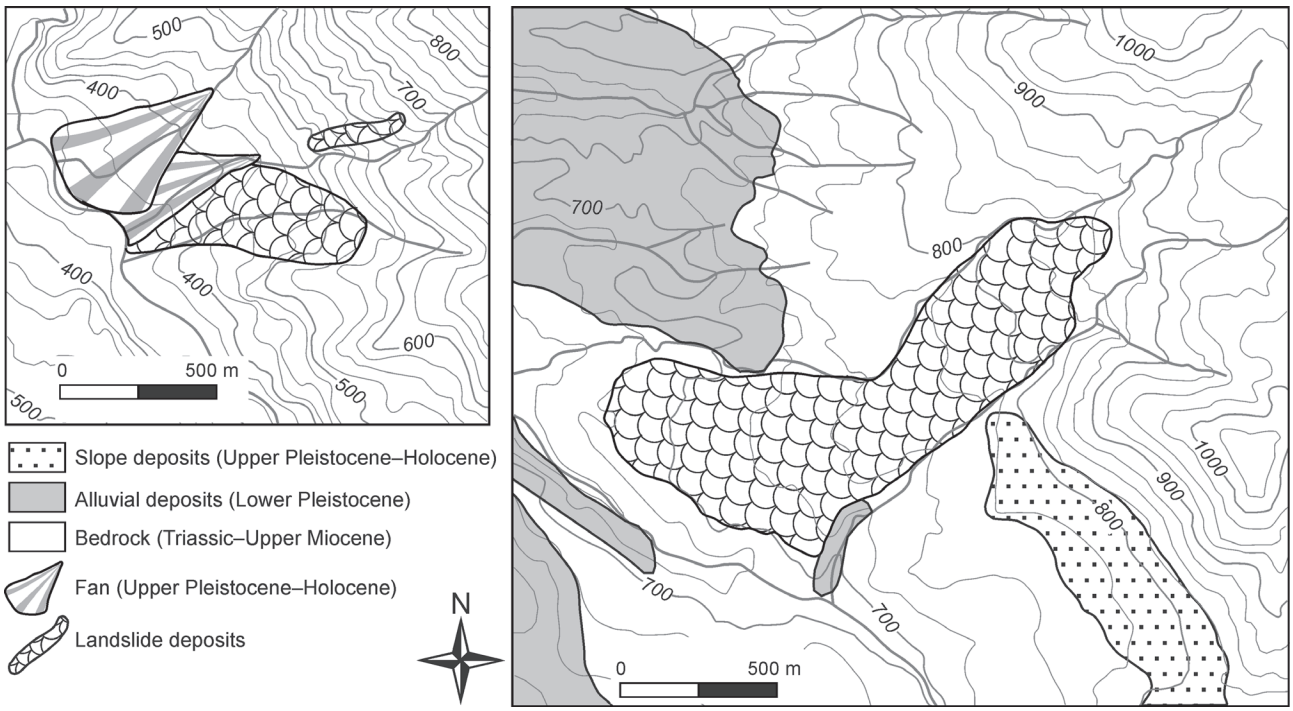

Fig. 2. Geological sketch maps of the studied landslides (see location in Fig. 1).

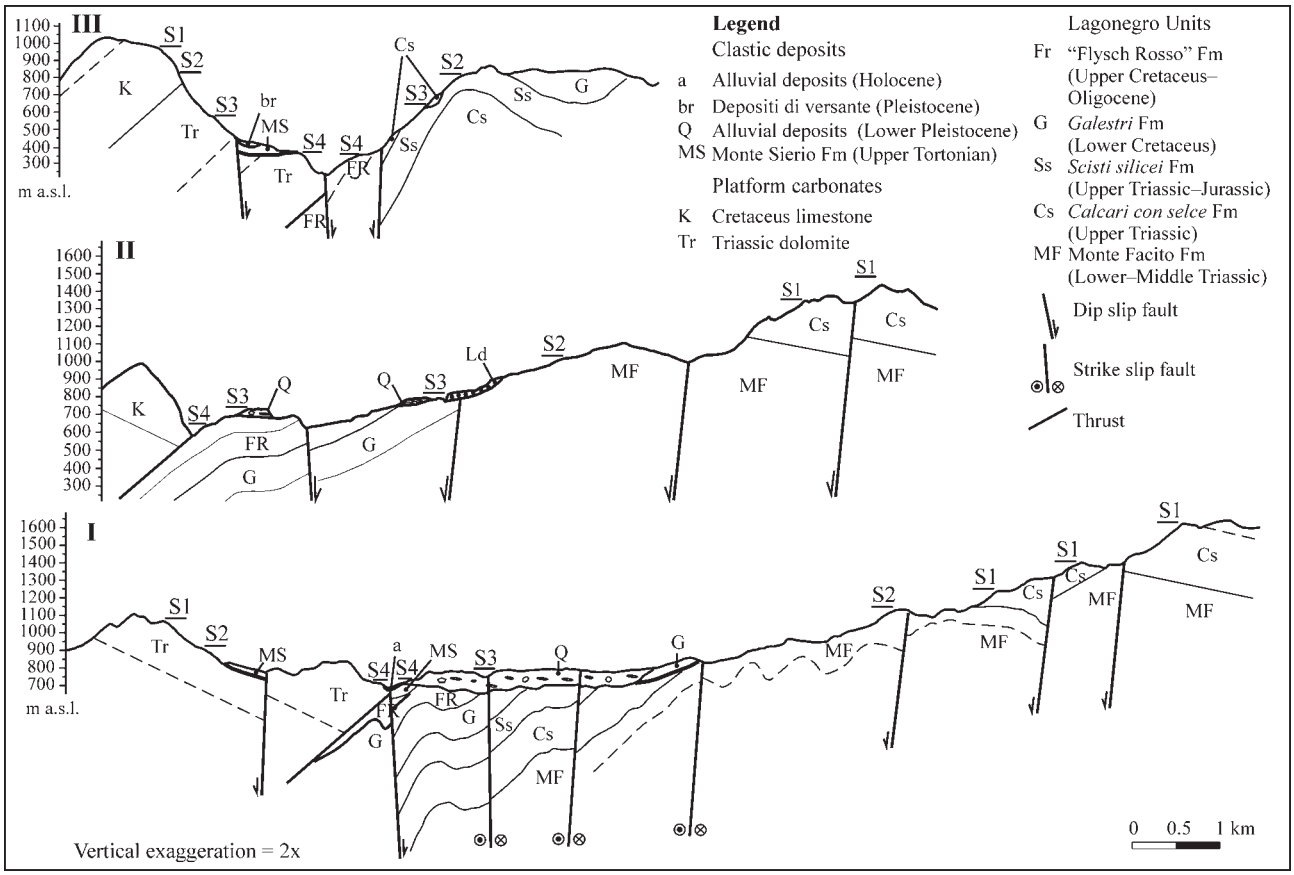

Fig. 3. Morphostratigraphic sections through the Melandro River basin, showing the relationships between faults, erosional surfaces, and paleo-landslides (see Fig. 1 for the location of the sections).

Fig. 4. Paleo-landslide (marked by the dashed line) and S3 erosional land surfaces (marked by the dotted lines) in the southern area of the Melandro basin. The S3 land surface cuts the intermediate sector of the landslide.

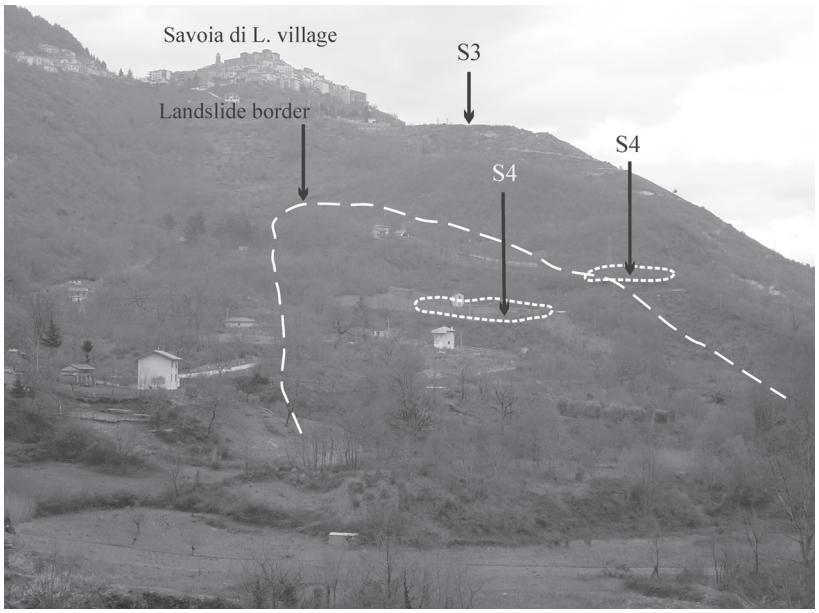

Fig. 5. Relationships between S3 and S4 erosional land surfaces and the paleo-landslide located in the northern part of the basin.

In the area of the Melandro River basin, two large landslides exhibiting peculiar characteristics have been mapped (Fig. 2) using modern criteria (Parise 2001, and references therein) and classified following the internationally accepted schemes (Varnes 1978; Cruden & Varnes 1996). Both the landslides have to be ascribed to deep-seated roto-translational rock slides and are 0.12 and 0.7 km^2 in size, respectively, in the northern and southern sectors of the valley (Fig. 1). The larger landslide developed into earth flows in its frontal part. Mass movements probably affected weathered rocks, as shown by some landslide deposit features. The same deposits are cut by erosional surfaces which are in turn deeply weathered.

In both cases, the landslide deposits are characterized by large rock blocks and fragmented beds dispersed in a fine-grained matrix. The rock blocks and beds belong to formations (i.e. Scisti silicei Formation and Calcari con selce Formation, Lagonegro units — Pescatore et al. 1999, and references therein; see also Di Leo et al. 2002 and Tanner et al. 2006) which are rarely involved in bedrock slide in the present-day geomorphic system. In addition, the size of the landslides, the thickness of the landslide deposits, and the dimensions of the blocks are not common features in recent mass movements of the southern Apennines.

The age of the paleo-landslides has been determined considering the relationships with the Quaternary deposits and the related landscapes. In the southern area of the basin a wide paleo-landslide, whose middle portion is cut by a remnant of the Middle Pleistocene land surface (Fig. 3, morpho-stratigraphic section in the middle, and Fig. 4), is recognizable. Furthermore, this paleo-landslide formed a morphological high separating different sectors of the basin in which Lower Pleistocene sediments were confined. After a successive stage of aggradation of the Melandro River paleo-valley, the landslide was partly "drowned" by alluvial sediments and successively planated together with the same fluvial deposits in response to a further change of the local base level of the erosion. The progressive fall of the local base level led to the vertical incision of the ancient (i.e. Early–Middle Pleistocene) alluvial plain, isolating large remnants of the S3 erosional land surface — sculptured both in bedrock and Quaternary (alluvial and landslide) deposits — and exhuming also the lower part of the paleo-landslide. Based upon this evidence, the landslide can be ascribed to the upper part of the Lower Pleistocene, which is the age of the uppermost portion of the fluvial succession.

Another paleo-landslide has been recognized in the northern sector of the basin (Fig. 1). It is "morphologically inserted" inside the Upper Pleistocene land surfaces (i.e. the landslide deposits are placed on a topography modelled below the erosion base level related to that order of land surfaces) and fossilized by fan deposits and small erosional surfaces located 25 m

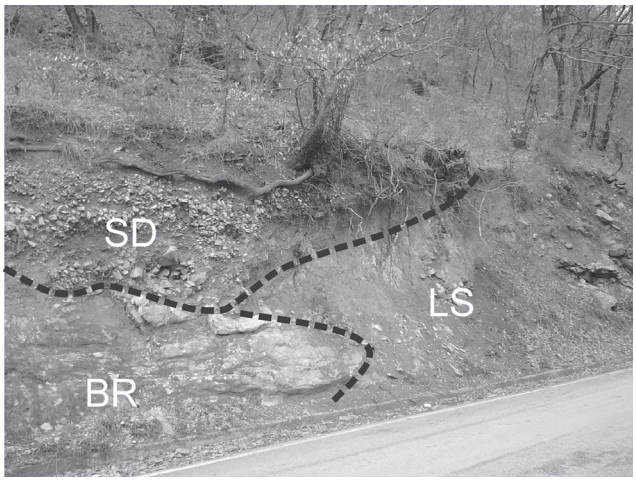

Fig. 6. Stratigraphic relationships between bedrock (BR), landslide (LS) and slope (SD) deposits in the northern sector of the studied area.

above the present-day valley floor (Fig. 5). Further, another close and similar landslide deposit is fossilized by slope deposits incised and suspended on the present-day thalweg (Fig. 6). On this basis, the age of the second paleo-landslide can be ascribed to the beginning of the Late Pleistocene.

Mineralogy and geochemistry

Materials and methods

In the present work the mineralogy and geochemistry of six samples from weathered horizons and landslides deposits have been investigated. ALT1 and ALT3 samples are from weathered horizons developed on a bedrock constituted by the Galestri Formation (Lower Cretaceous) and sculptured by the third order erosional surface S3. ALT2 sample is from a weathered horizon developed on the bedrock constituted by Scisti silicei Formation (Jurassic–Upper Triassic), and ALT6 sample belongs to a weathered horizon developed on Flysch Rosso Formation (Oligocene–Upper Cretaceous). ALT4 and ALT5 represent landslide deposits. The mineralogy of the bedrocks is described in Di Leo et al. (2002) and for sake of simplicity is summarized in the present paper in Fig. 7.

The mineralogical associations in the selected samples were identified by X-ray diffraction using a Rigaku miniflex apparatus, operating under the following conditions: CuK_{α} radiation, 0.02 steps, 0.5°/min time, sample spinner. The XRD analysis was carried out on powders crushed in an *agate* hand mortar. To identify clay minerals, a known amount of the <2 μm grain-size fraction — isolated through settling after dispersion in deionized water — was dried at room temperature and pipetted on glass slides to produce a well-oriented specimen. Air-dried, ethylene-glycol solvated, heated (250 °C, 375 °C, 500 °C) and Mg-saturated mounts were X-rayed. The MacDiff software (4.2 version), with JCPDS mineralogical cards database, was used to identify the mineralogical phases. The "illite crystallinity", expressed as the Kübler Index (KI; Kübler 1964) and calibrated to the *CSI scale* (*Calibration Standards Index scale*, Warr & Rice 1994), and the "kaolinite crystallinity", expressed as Hinckley Index (HI; Hinckley 1963) have also been measured. The distribution of mineralogical phases (expressed in weight %) of studied weathered horizons and landslides deposits samples are showed in Fig. 8.

Major elements abundances (expressed weight % of oxides) in the weathered horizons and landslide deposits were estimated by X-ray fluorescence (XRF). Total loss on ignition (LOI) was gravimetrically estimated after overnight heating at 950 °C. Geochemical data together with weathering indexes, i.e. *Chemical Index of Alteration* (CIA*;* Nesbit & Young 1982) and *Weathering Ratio* (WR; Chittleborough 1991) are showed in Table 1. The CIA represents the:

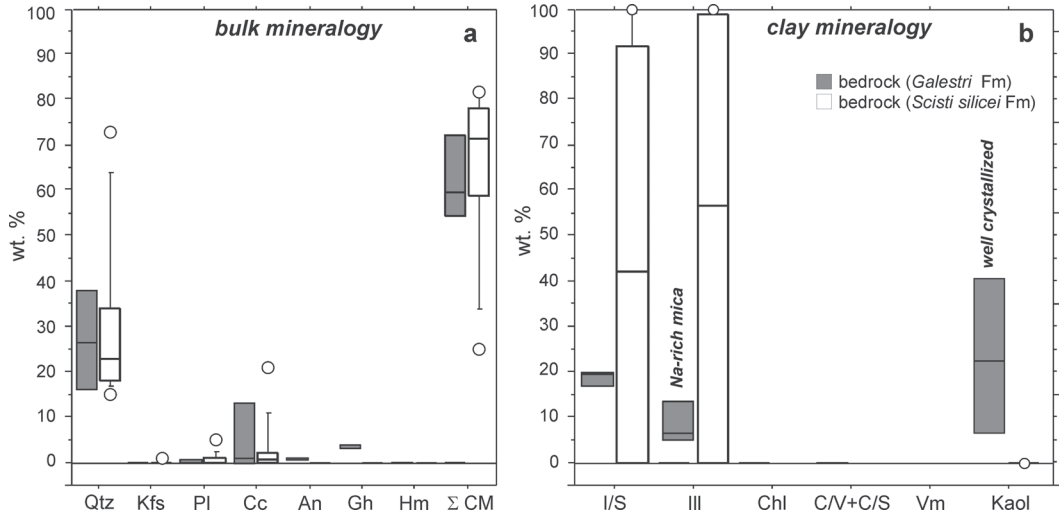

Fig. 7. Distribution of the mineralogical phases (expressed in weight %) in pelitic levels from the Scisti silicei and Galestri Fms (data from Di Leo et al. 2002) which represent the bedrock of the studied weathered horizons. **a** — Qtz = quartz, Pl = plagioclases, Kfs = K-feldspars, Cc = calcite, An = anatase, Gh = goethite, Hm = hematite, Σ CM = sum of clay minerals. **b** — Chl = chlorite, I/S = illite/smectite mixed layers, C/V = chlorite/vermiculite mixed layers, C/S = chlorite/smectite mixed layers, Kaol = kaolinite, Ill = illite, Vm = vermiculite.

$$\left[\frac{Al_2O_3}{(Al_2O_3 + CaO^* + Na_2O + K_2O)}\right]^*100 \quad \text{ratio,}$$

where the CaO* represents the CaO associated with the silicate fraction of the sample, and the WR is estimated by normalizing the sum of the mobile elements ($CaO^* + Na_2O + MgO$) to the immobile element TiO_2.

Results

The mineral association identified in the landslide deposit (ALT4) and weathering horizons (ALT1 and ALT3) developed on the Galestri Formation is mainly constituted by clay minerals (75–69 %), quartz (9–16 %), calcite (< 10 %), and traces of plagioclases, K-feldspars and anatase (Fig. 8). Goethite has also been identified, although in a low amount (< 3 %), in these samples. Among clay minerals, illite/smectite mixed-layers with a 60–70 % of illitic layers (I/S_{ill}, R1; Reynolds 1985) are the most abundant (46–63 %), together with chlorite/vermiculite and chlorite/smectite (C/V and C/S respectively). Illite content is variable (9–44 %), and its KI — ranging between 0.69 and 0.86 Δ°2θ — indicates the presence of a mainly poorly crystallized non-expandable 10 Å phase. Kaolinite (7–18 %) also exhibits a low degree of "crystallinity" according to the low Hinckley Index values (0.17 and 0.20). Besides, the position in the XRD patterns of its $d_{(001)}$ reflection at 7.2 Å — that shifts near to 8.0 Å after treatment with ethylene-glycol — indicates the presence of little mixed-layering with "chloritized" smectite. A great amount of vermiculite (14 %) has been identified only in the ALT3 sample. The presence in the XRD patterns of oriented mounts, heated at 350° and 550 °C for 1 hour, of two large peaks at about 13 Å and 11.8 Å and the comparison with XRD pattern of the Mg-saturated mount, suggests the presence of a 2 : 1 mineralogical phase like Al-rich vermiculite (Taveldal et al. 1990).

Samples from the weathered horizon developed on Scisti silicei Formation (ALT2) and from landslide deposit (ALT5) are constituted by clay minerals (47–51 %), quartz (47 %), and traces of plagioclases and hematite (Fig. 8). Among the clay minerals, illite, with a KI value ranging from 0.77 to 0.86 Δ°2θ is the most abundant clay mineral (20–27 %), together with illite/smectite mixed layers (18 % in ALT2) with 70 % of illitic layers (I/S_{ill}, R1; Reynolds 1985) and chlorite/vermiculite (20 % in ALT5) mixed layers. Kaolinite (10 %) is poorly crystallized, as suggested by Hinckley Index value (HI = 0.15). Also for these samples the position in the XRD patterns of the its $d_{(001)}$ reflection at 7.2 Å — that shifts near

Table 1: Distribution of main oxides (weight %) in samples of weathered horizons and landslide deposits.

Sample	ALT1	ALT2	ALT3	ALT4	ALT5	ALT6
SiO_2	55.75	71.85	52.27	48.79	70.23	21.13
TiO_2	1.16	0.39	0.81	1.27	0.62	0.46
Al_2O_3	20.69	12.02	17.21	23.15	13.15	7.65
FeO	0.35	0.15	1.66	0.57	0.13	0.62
Fe_2O_3	6.56	3.62	4.60	4.31	4.36	2.99
MnO	0.18	0.01	0.08	0.04	0.32	0.08
MgO	1.17	0.77	2.08	0.68	1.82	1.94
CaO	1.11	0.21	3.92	5.37	0.49	29.67
Na_2O	0.80	0.10	1.02	0.97	0.49	0.15
K_2O	1.92	1.64	3.63	1.77	3.18	1.03
P_2O_5	0.15	0.05	0.14	0.10	0.09	0.21
LOI	11.08	7.21	9.64	14.55	6.07	29.15
CIA	86	86	79	89	76	87
WR	2.180	2.769	3.813	1.302	4.502	4.524

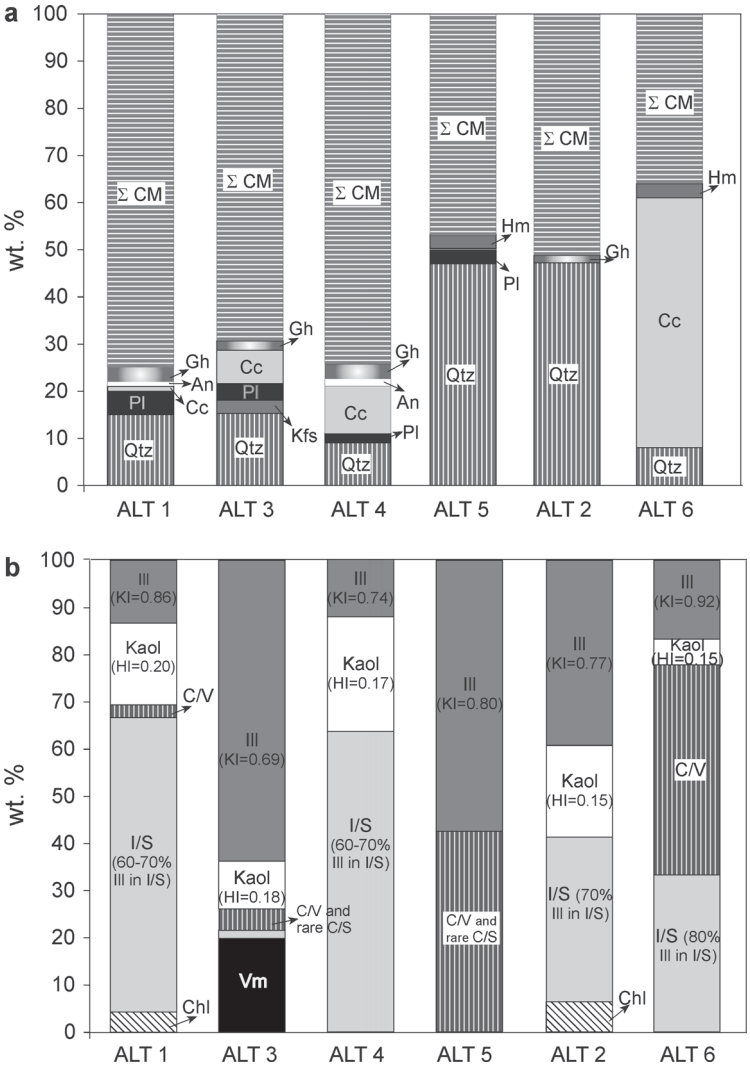

Fig. 8. Distribution of the mineralogical phases (expressed in weight %) identified in the studied weathered horizons and landslide deposits. **a** — Qtz = quartz, Pl = plagioclases, Kfs = K-feldspars, Cc = calcite, An = anatase, Gh = goethite, Hm = hematite, Σ CM = sum of clay minerals. **b** — Chl = chlorite, I/S = illite/smectite mixed layers, C/V = chlorite/vermiculite mixed layers, C/S = chlorite/smectite mixed layers, Kaol = kaolinite, Ill = illite, Vm = vermiculite. KI is the Kübler Index (Kübler 1964), HI is the Hinckley Index (Hinckley 1963).

to 8.0 Å after treatment with ethylene-glycol — suggests the presence of a little mixed-layering with "chloritized" smectite.

In the sample from the weathered horizon developed on the Flysch Rosso Formation (ALT6), calcite (53 %), clay minerals (36 %), quartz (8 %) are the main mineralogical phases. Traces of hematite are also present in the sample. Interstratified chlorite/vermiculite and illite/smectite with 80 % of illitic layers (I/S_{ill}, R1; Reynolds 1985) are the most abundant clay minerals (15 % and 12 %, respectively). Both illite (6 %) and kaolinite are poorly crystallized as suggested by the KI and HI indexes equal to 0.92 $\Delta°2\theta$ and 0.15, respectively.

Paleoclimate implications

The peculiar mineralogical associations observed in the sampled weathered horizons, compared to their relative bedrocks represented by the Scisti silicei and Galestri Formations, suggest that the alteration developed through two main stages related to different paleoclimate scenarios (Fig. 9). In the bedrocks on which the analysed weathered horizons developed, minerals such as vermiculite and chlorite/vermiculite interlayers are totally absent (Fig. 4). Therefore, the formation in the weathered horizons of such minerals, most probably at the expense of mica (the Scisti silicei and Galestri Formations contain a well crystallized Na-rich mica; Di Leo et al. 2002), is likely to be the result of weathering developed in a cold-temperate climate setting, with an alternation of rainy seasons — where an intense leaching occurred — and dry periods. Semi-arid climate, with dry/humid periods, is a necessary condition for the formation of vermiculite at the expense of mica (Scott & Smith 1968; Righi & Meunier 1995). During dry seasons, K^+ ions are in fact expelled from the interlayer region of mica (a 2 : 1 clay mineral) and, because of the leaching, is definitively removed to form vermiculite (a 2 : 1 : 1 clay mineral). The alternation of dry and humid climate periods (aerobic/anaerobic cycles) is a necessary condition for the disappearance of 2 : 1 clay minerals and the appearance of the newly formed 2 : 1 : 1 Al- and Mg-rich "chloritized" mineral phases (Schaetzl & Anderson 2005). Intense leaching joined to the weak soil acidity and low organic matter lead to the formation of both pedogenic chlorite and Al-rich vermiculite (Rich 1968; Barnhisel & Bertsch 1989).

The recognition of poorly crystallized kaolinite and goethite in the analysed weathering horizons as well as of kaolinite/smectite mixed-layers (K/S), which were not observed in the bedrocks on which they developed (Fig. 4) — kaolinite is only observed in correlated levels within the Galestri Formation, where it exhibits a high crystallinity, and is totally absent in analogously correlated levels within the Scisti Silicei Formation (Di Leo et al. 2002; Schiattarella et al. 2003, 2006) — suggest that a more intense weathering period has also contributed to the formation of these weathered horizons and that a change to climate conditions typical of a mainly warm/humid climate occurred (Fig. 9). The K/S formation is in fact generally associated with the formation of soils in warm/humid climate contexts, and represents an important stage of kaolinite formation (Bhattacharyya et al. 2006).

However, the co-existence of newly formed minerals linked to weathering developed in a mainly cold/temperate climate setting with those typical of a stage of alteration developed in warm/humid conditions

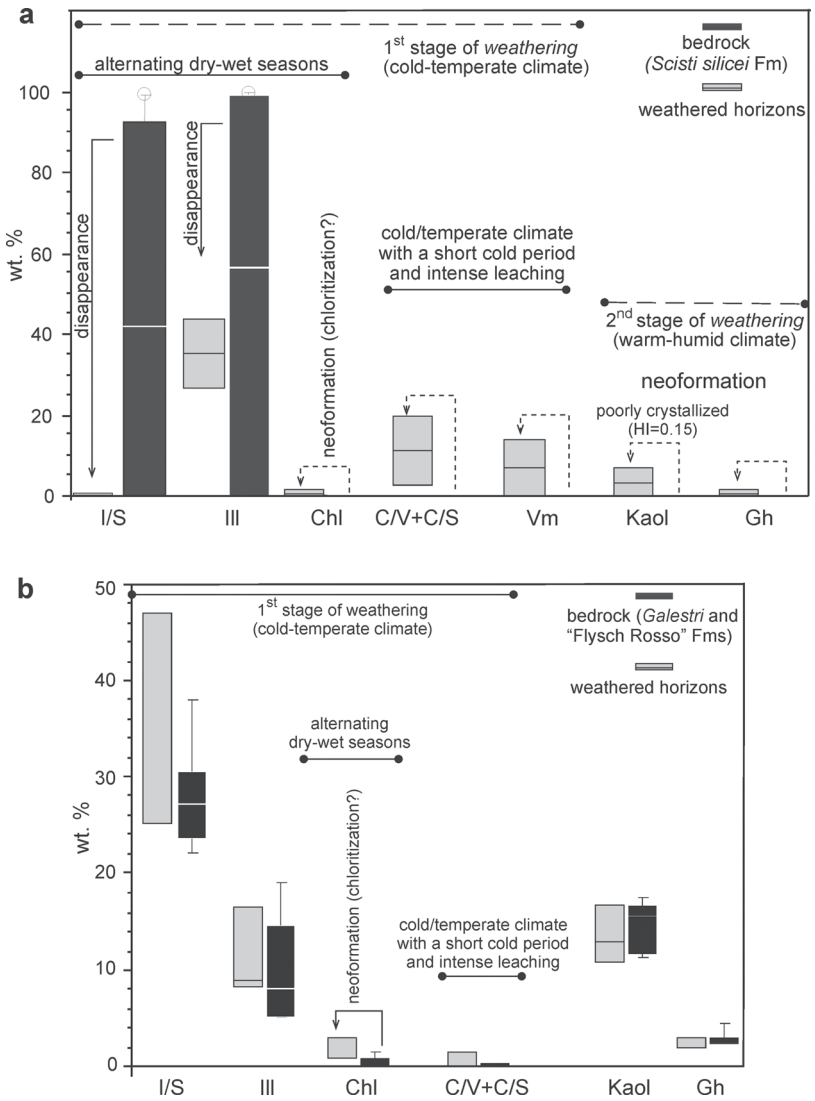

Fig. 9. Mineralogical associations recognized in the weathered horizons and relative to different weathering stages characterized by different paleoclimate conditions (mineralogical phase labels as indicated in Fig. 6). For comparison, the mineralogical features of the bedrocks on which the horizons developed belonging to the Scisti silicei (**a**), Galestri and Flysch Rosso Formations (**b**) are also reported (data from Di Leo et al. 2002 and Schiattarella et al. 2003).

clearly suggests that the latter stage, although intense, must have lasted for a relatively short time span. Therefore, vermiculite, C/V and C/S interlayers were still preserved and coexisted with newly formed kaolinite and K/S interlayers.

Using a multivariate statistical approach, carried out by the *Principal Component Analysis* (PCA) method (Fig. 10), the distribution of the mineralogical phases in the weathering horizons were compared to the ones in the bedrock on which the horizons developed (data from Di Leo et al. 2002). This allowed us to clearly identify the two main weathering stages related to different paleoclimate scenarios that are responsible for the development of the weathered horizons (see Fig. 10). The first component (29% of explained variance), with high positive *component loadings*, group together kaolinite and goethite abundance normalized to quartz $\left(\frac{gh+kaol}{qtz}\right)$. This component indicates the stage of weathering related to a humid/warm climate context. The second component (23 % of explained variance), with high positive *component loadings*, grouping together variables such as vermiculite, chlorite, and chlorite/smectite mixed layers abundances, normalized to quartz $\left(\frac{vm+chl+C/S}{qtz}\right)$, identifies the stage of the alteration developed in a cold/temperate climate context, characterized by alternation of wet seasons and dry periods (presence of vermiculite). The 1st component *versus* 2nd component plot (Fig. 10) depicts an area where all the analysed weathered horizons produced by the onset of two different climate settings fall, with CIA values >85 (Nesbit & Young 1982). The altered samples are far away from areas where their relative bedrocks are located. These are respectively placed in the direction of maximum variation of quartz and illite (mineralogical phases that predominate in samples from Scisti silicei Formation) and of illite/smectite mixed layers and well crystallized kaolinite (mineralogical phases that predominate in samples from Galestri and Flysch Rosso Formations). Sample ALT5 was the least-altered sample for it falls within the group of the unaltered bedrock constituted by the Scisti silicei Formation.

Similar considerations can be drawn from the analysis of the geochemical features of both the landslide deposits and the weathered horizons. The variation plot (Fig. 11) of the CIA *vs.* the WR indexes is also evidence of the evolutionary trend of weathering where ALT3 and ALT5 represent the less altered samples, closer to the original composition of their relative bedrocks, namely the Galestri and Scisti silicei Formations respectively.

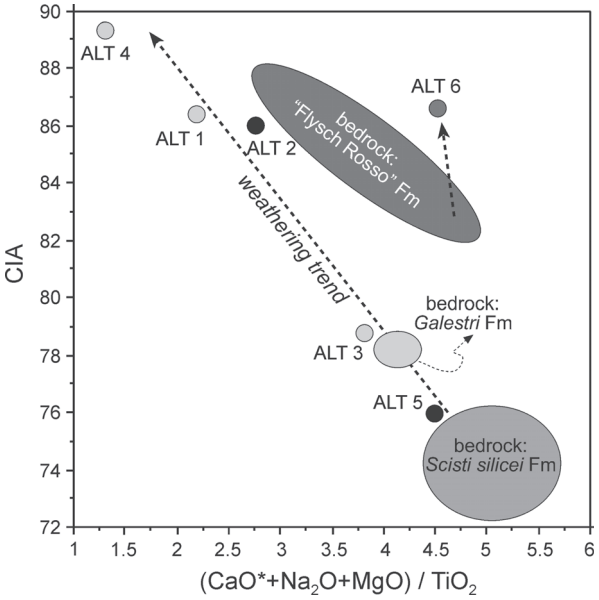

Fig. 11. Variation plot of CIA (Chemical Index of Alteration) *versus* WR (Weathering Ratio; Chittleborough 1991). CIA is the $\left[\frac{Al_2O_3}{(Al_2O_3+CaO^*+Na_2O+K_2O)}\right]*100$ ratio (where the CaO* represents the CaO associated with the silicate fraction of the sample) and the WR is estimated by normalizing the sum of the mobile elements (CaO^*+Na_2O+MgO) to the immobile element TiO_2 (data for bedrocks formations from Di Leo et al. 2002).

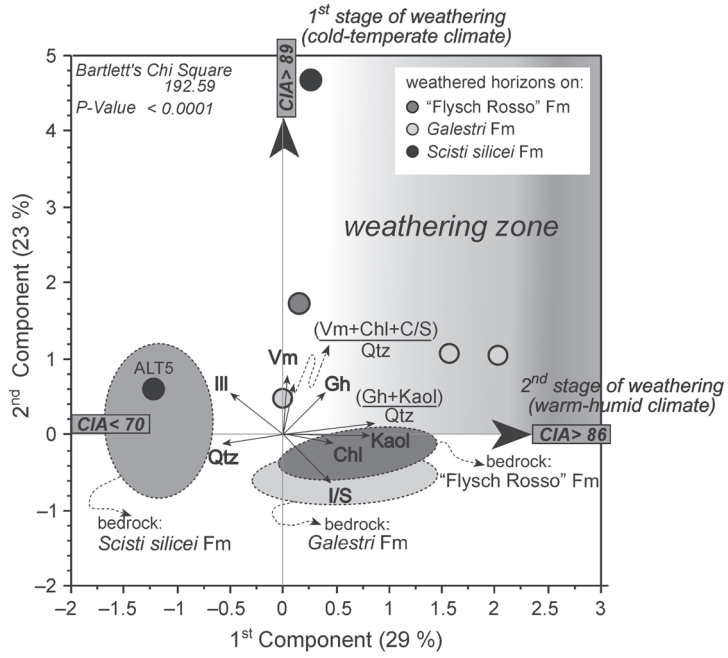

Fig. 10. Orthogonal plot relative to the multivariate statistical analysis carried out on mineralogical variables represented by the abundances of mineral phases identified in the analysed samples, and their relative ratios, using the *Principal Component Analysis* (PCA) method to extract components (for the description of mineralogical phases labels see Fig. 6). Mineralogical data for bedrocks, represented by Scisti silicei, Galestri and Flysch Rosso Formations, are from Di Leo et al. (2002) and Schiattarella et al. (2003). For analytical CIA values (Chemical Index of Alteration) see Table 1.

Discussion and conclusions

Uplift rates have been calculated using geomorphological, stratigraphical and structural data.

Geomorphic data consist essentially of elevation values, ages and arrangement of erosional gently dipping land surfaces and other morphotectonic indicators such as suspended valleys, gorges, convex slopes, and strath terraces (Burbank & Anderson 2001). The morphostructural evolution of the Melandro basin is characterized by stages of uplift alternated with slack periods in which the erosional surfaces developed. In particular, four orders of erosional surfaces have been detected through field survey and geomorphological analysis (Fig. 1). The relative age of these surfaces have been defined on the basis of morphostratigraphic relationships with Pliocene to Quaternary deposits. Specifically, the oldest paleosurface (S1) cuts the Pliocene deposits at the tops of the Maddalena Mountains whereas the intermediate surface (S3) cuts the Lower Pleistocene deposits filling the main depression of the Melandro River basin (Fig. 3). Another order of erosional flat surfaces (S2) is interposed between the oldest and intermediate surfaces: its morphostratigraphic position suggests that the genesis of this erosional landscape occurred in the Early Pleistocene. Finally, the youngest surface (S4) is Middle–Late Pleistocene in age, as verified for similar terraces in adjacent areas (Schiattarella et al. 2003). Local, less extended, fluvial terraces (S5) are also present in the basin. The relative ages of the different land surface orders (here assumed as the tectonic episodes causing the morphological de-activation of a paleosurface order as an ancient base level of erosion) have been established on the basis of the record of the well-known regional tectonic stages found in southern Italy (Schiattarella et al. 2006, and references therein).

Local uplift rates have been estimated using the difference in height between the local erosion base levels (i.e. present-day thalwegs) and the several generations of land surfaces (Table 2), whereas the stage (or partitioned) uplift rates (cf. Schiattarella et al. 2006) have been calculated on the basis of the difference in elevation between a given order of land surfaces and that immediately younger, with the aim of consid-

Table 2: Morphometric characters of land surfaces from the Melandro basin area and ages of their morphological de-activation (i.e. starting of tectonic uplift), with related values of local and stage uplift rates.

Erosional surface	Age (Ma)	Elevation range (m)	Local uplift rate (mm/yr)	Stage uplift rate (mm/yr)
Western flank of the basin				
S1	1.8	1100–1300	0.35	0.34
S2	1.2	900–1000	0.36	0.43
S3	0.73	800–600	0.26	0.27
S4	0.125	500–550	0.39	0.42
Eastern flank of the basin				
S1	1.8	1400–1600	0.46	0.61
S2	1.2	950–1100	0.40	0.64
S3	0.73	800–600	0.22	0.18
S4	0.125	500–550	0.39	0.42

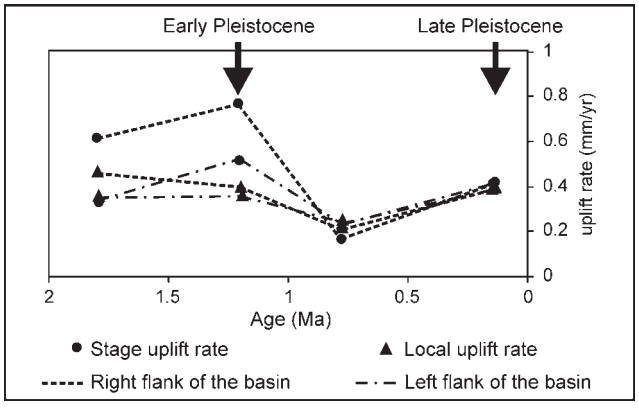

Fig. 12. Local and stage uplift rates based on the morphological de-activation (i.e. tectonic uplift) ages of the land surfaces.

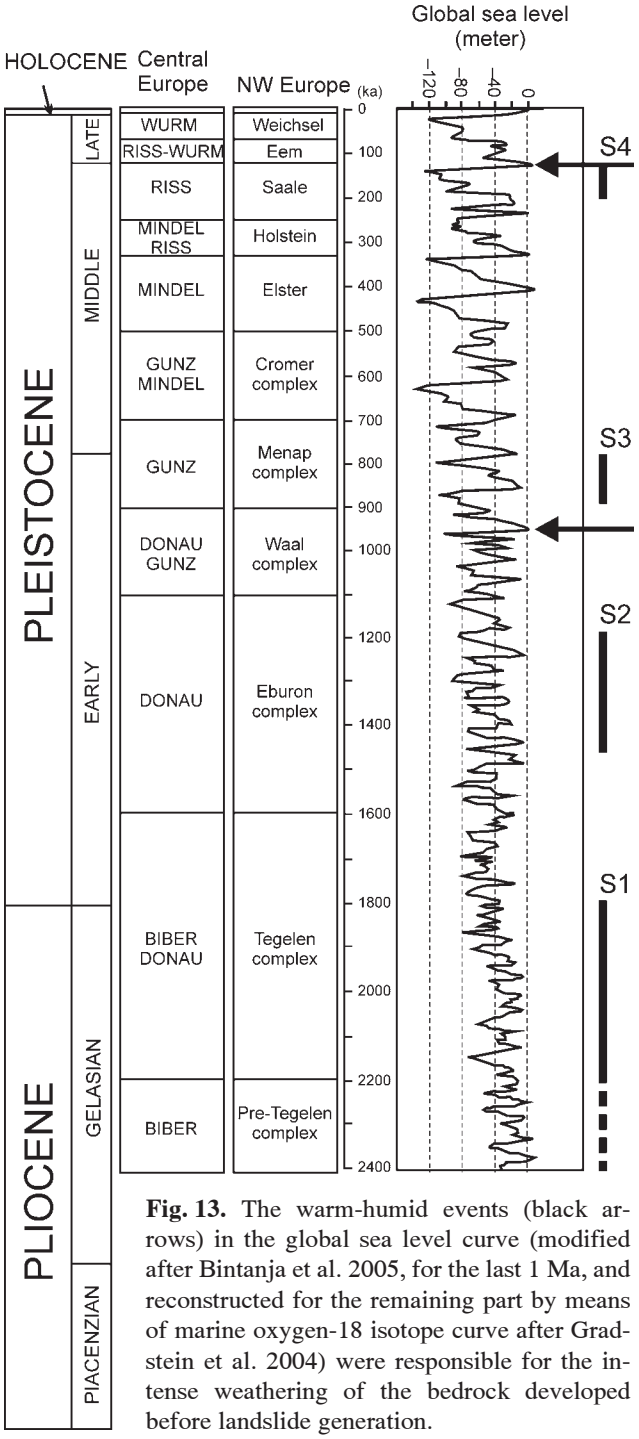

Fig. 13. The warm-humid events (black arrows) in the global sea level curve (modified after Bintanja et al. 2005, for the last 1 Ma, and reconstructed for the remaining part by means of marine oxygen-18 isotope curve after Gradstein et al. 2004) were responsible for the intense weathering of the bedrock developed before landslide generation.

ering the trend in specific time intervals. In the study area, the stage uplift is characterized by two velocity increments: the first during the upper part of the Early Pleistocene and the second during the Late Pleistocene (Fig. 12).

The mineralogical associations identified in the analysed landslide deposits and weathered horizons, and comparison with the original composition of the rocks that represents the bedrock on which they developed, suggest that the weathering conditions evolved through two main stages related to different paleoclimate scenarios (see Figs. 10 and 11). Climate conditions changed from a relatively cold/temperate scenario, characterized by the alternation of dry/wet seasons, where a less intense weathering developed (CIA ~76 and WR ~4.5), to a more warm/humid setting in which the weathering of the bedrock was more pronounced (CIA 80–90 and WR <3.7). The warmer climate stage, although intense, must have lasted for a relatively short time so that the mineralogical association developed during the relatively cold/temperate climate was still preserved in the analysed weathered horizons.

The ages of the paleo-landslides surveyed in the Melandro basin were determined on the basis of geomorphological observations and other chronological constraints, such as the presence of Quaternary deposits cut by the same erosional surfaces affecting the ancient landslides. The correlation between the assigned ages of such paleo-landslides and the temporal trend of the stage uplift rates allowed us to hypothesize that the landslides occurred in response to peaks in the tectonic uplift. During these peaks, strong earthquakes were probably more frequent and the mountain slopes were therefore destabilized by the rapid relief growth. On the other hand, the peculiar features of the slide material seem to be due to the deep weathering of the bedrock during a warm-humid climate stage (Fig. 13) and before the tectonic events, as shown by two positive peaks in the most recent reconstructions of the Quaternary global sea-level changes (Gradstein et al. 2004; Bintanja et al. 2005). It is remarkable to note that the oldest peak, included in the Donau-Günz interglacial stage, coincides with the formation of a sapropel, widely diffused in the Mediterranean area, with an age spanning from 960 to 955 ka (Meyers & Arnaboldi 2005), whereas the youngest peak represents the debut of the Riss-Würm interglacial stage at the beginnings of the Late Pleistocene.

Acknowledgments: This study was financially supported by *Fondi di Ateneo* 2007 and 2008 (Basilicata University) grants (Professor M. Schiattarella). We wish to thank Professor Brian Whalley and Professor Alice Turkington for their useful comments and suggestions in reviewing the manuscript.

References

Amato A. & Cinque A. 1999: Erosional landsurfaces of Campano-Lucano Apennines (S. Italy): genesis, evolution and tectonic implications. *Tectonophysics* 315, 251–267.

Barnhisel R.I. & Bertsch P.M. 1989: Chlorites and hydroxy-interlayered vermiculite and smectite. In: Dixon J.B. & Weed S.B. (Eds.): Minerals in soils environments. *Soil Sci. Soc. Amer.*, Madison, WI, 2nd edn., 729–788.

Bhattacharyya T., Pal D.K. & Deshpande S.B. 2006: Genesis and transformation of minerals in the formation of red (Alfisols) and black (Inceptisols and Vertisols) soils on Deccan basalt in the Western Ghats, India. *European J. Soil Sci.* 44, 159–171.

Bintanja R., van de Wal R.S.W. & Oerlemans J. 2005: Modelled atmospheric temperature and global sea levels over the past million years. *Nature* 437, 125–128.

Bloom A.L. 1978: Geomorphology: A systematic analysis of Late Cenozoic landforms. *Prentice-Hall*, Englewood Cliffs, 1–510.

Bordoni P. & Valensise G. 1998: Deformation of the 125 ka marine terrace in Italy: tectonic implications. In: Stewart I. & Vita-Finzi C. (Eds.): Late Quaternary coastal tectonics. *Geol. Soc. London, Spec. Publ.* 146, 71–110.

Brancaccio L., Cinque A., Romano P., Rosskopf C., Russo F., Santangelo N. & Santo A. 1991: Geomorphology and neotectonic evolution of a sector of Tyrrhenian flank of the southern Apennines (Region of Naples, Italy). *Z. Geomorphol., Suppl-Bd.* 82, 47–58.

Bull W.B. 1991: Geomorphic responses to climatic change. *Oxford University Press*, New York, 1–326.

Burbank D.W. & Anderson R.S. 2001: Tectonic geomorphology. *Blackwell Science*, Oxford, 1–274.

Chittleborough D.J. 1991: Indices of weathering for soils and paleosols formed on silicate rocks. *Australian J. Earth Sci.* 38, 115–120.

Cruden D.M. & Varnes D.J. 1996: Landslides types and processes. In: Turner A.K. & Schuster R.L. (Eds.): Landslides: Investigation and mitigation. *Transportation Research Board Special Report 247. National Academy of Sciences*, Washington, 36–75.

D'Argenio B., Ortolani F. & Pescatore T. 1986: Geology of southern Apennines. A brief outline. *Geologia Applicata e Idrogeologia* 21, 135–160.

Di Leo P., Dinelli E., Mongelli G. & Schiattarella M. 2002: Geology and geochemistry of Jurassic pelagic sediments, *Scisti silicei* Formation, southern Apennines, Italy. *Sed. Geol.* 150, 229–246.

Giano S.I. & Martino C. 2003: Morphostructural and morphostratigraphic setting of Pleistocene continental deposits of the Pergola-Melandro basin (Lucanian Apennine). *Quaternario* 16, 289–297 (in Italian).

Gradstein F.M. et al. 2004: A geologic time scale 2004. *Geol. Surv. Canada, Miscellaneous Report* 86, 1 (poster).

Hickley D. 1963: Variability in "crystallinity" values among the Kaolin deposits of the coastal plain of Georgia and South Carolina. *Clays and Clay Miner.* 11, 229–235.

Kübler B. 1964: Les argiles, indicateurs de métamorphisme. *Revue Instituté de la Francais de Pétrole* 19, 1093–1112.

Lippman Provansal M. 1987: L'Apennin méridional (Italie): étude géomorphologique. *Thèse de Doctorat d'Etat en Géographie Physique, Université d'Aix-Marseille*.

Martino C. & Schiattarella M. 2006: Morphotectonics and Quaternary geomorphological evolution of the Melandro Valley, southern Apennines, Italy. *Quaternario* 19, 119–128 (in Italian).

Meyers P.A. & Arnaboldi M. 2005: Trans-Mediterranean comparison of geochemical paleoproductivity proxies in a mid-Pleistocene interrupted sapropel. *Palaeogeogr. Palaeoclimatol. Palaeoecol.* 222, 313–328.

Nesbit H.W. & Young G.M. 1982: Early Proterozoic climates and plate motion inferred from major element chemistry of lutites. *Nature* 299, 715–717.

Ollier C.D. 1981: Tectonics and landforms. *Longman*, London and New York, 1–324.

Ortolani F., Pagliuca S., Pepe E., Schiattarella M. & Toccaceli R.M. 1992: Active tectonic in the southern Apennines: relationships between cover geometries and basement structure. A hypothesis for a geodynamic model. *IGCP No. 276*, Newsletter 5, 413–419.

Parise M. 2001: Landslide mapping techniques and their use in the assessment of the landslide hazard. *Physics and Chemistry Earth* 26, 697–703.

Pescatore T., Renda P., Schiattarella M. & Tramutoli M. 1999:

Stratigraphic and structural relationships between Meso-Cenozoic Lagonegro basin and coeval carbonate platforms in southern Apennines, Italy. *Tectonophysics* 315, 269–286.

Reynolds R.C. Jr. 1985: NEWMOD a computer program for the calculation of one-dimension diffraction patterns of mixed-layered clays. *R.C. Reynolds, Jr., 8 Brook Dr., Hanover*, New Hampshire.

Rich C.I. 1968: Hydroxy interlayers in expansible layer silicates. *Clays and Clay Miner.* 16, 15–30.

Righi D. & Meunier A. 1995: Origin of clays by rock weathering and soil formation. In: Velde B. (Ed.): Origin and mineralogy of clays. *Springer*, Berlin, 43–157.

Schaetzl R.J. & Anderson S. 2005: Soils: Genesis and geomorphology. *Cambridge University Press*, New York, 1–817.

Schiattarella M. 1998: Quaternary tectonics of the Pollino Ridge, Calabria-Lucania boundary, southern Italy. In: Holdsworth R.E., Strachan R.A. & Dewey J.F. (Eds.): Continental transpressional and transtensional tectonics. *Geol. Soc. London, Spec. Publ.* 135, 341–354.

Schiattarella M., Di Leo P., Beneduce P. & Giano S.I. 2003: Quaternary uplift vs tectonic loading: a case-study from the Lucanian Apennine, southern Italy. *Quat. Int.* 101–102, 239–251.

Schiattarella M., Di Leo P., Beneduce P., Giano S.I. & Martino C. 2006: Tectonically driven exhumation of a young orogen: an example from the southern Apennines, Italy. In: Willett S.D., Hovius N., Brandon M.T. & Fisher D. (Eds.): Tectonics, climate, and landscape evolution. *Geol. Soc. Amer.*, *Spec. Pap.*, 398, *Penrose Conference Series*, 371–385.

Scott A.D. & Smith S.J. 1968: Mechanism for soil potassium release by drying. *Soil Sci. Soc. Amer. J.* 32, 443–444.

Summerfield M.A. 2000: Geomorphology and global tectonics. *Wiley*, Chichester, 1–367.

Tanner L.H., Schiattarella M. & Di Leo P. 2006: Carbon isotope record of Upper Triassic strata of the Lagronegro Basin, Southern Apeninnes, Italy: preliminary results. In: Harris et al. (Eds.): The Triassic–Jurassic terrestrial transition. *New Mexico Mus. Nat. His. Sci. Bull.* 37, 23–28.

Teveldall S., Jørgensen P. & Stuanes A.O. 1990: Long-term weathering of silicates in a sandy soil at nordmoen, Southern Norway. *Clay Miner.* 25, 447–465.

Varnes D.J. 1978: Slope movements types and processes. In: Schuster R.L. & Krizek R.J. (Eds.): Landslides: Analysis and control. *Transportation Research Board Special Report 176 National Academy of Sciences*, Washington, 11–33.

Warr A.W. & Rice A.H.N. 1994: Interlaboratory standardization and calibration of clay mineral crystallinity and crystallite size data. *J. Metamorph. Geology* 12, 141–152.

Westaway R. 1993: Quaternary uplift of Southern Italy. *J. Geophys. Res.* 98, 21741–21772.

Widdowson M. 1997: Palaeosurfaces: Recognition, reconstruction and palaeoenvironmental interpretation. *Geol. Soc. London, Spec. Publ.* 120, 330.

Willett S.D., Hovius N., Brandon M.T. & Fisher D. 2006: Tectonics, climate, and landscape evolution. *Geol. Soc. Amer., Spec. Pap.*, 398, *Penrose Conference Series*, 1–447.